archaeometry

Archaeometry ••, •• (2019) ••–•• doi: 10.1111/arcm.12456

NMR AS A NEW TOOL FOR CULTURAL HERITAGE APPLICATION: THE PROVENANCE OF ANCIENT WHITE MARBLES*

A. GUTIÉRREZ GARCIA-M.,[1,2] M. C. SAVIN,[1] N. CANTIN,[1] S. BOUDOUMI,[1] P. LAPUENTE,[2,3] R. CHAPOULIE[1] and I. PIANET[1]†

[1]*IRAMAT CRP2A, UMR 5060, CNRS, Université Bordeaux Montaigne, Maison de l'Archéologie, Esplanade des Antilles F-33607 Pessac, France*

[2]*ICAC, Plaça d'en Rovellat E-43003 Tarragona, Spain*

[3]*Departamento de Ciencias de la Tierra, Área de Petrología y Geoquímica, Facultad de Ciencias, Universidad de Zaragoza, Zaragoza, Spain*

Identifying the origin of marble used in antiquity brings back to light details of the economic, social and political organization of classical societies, and characterizing in depth the chemistry of marble is key to discovering its provenance. Beyond X-ray diffraction, which could reveal the presence of discriminant secondary crystalline phases and the quantification of accessory minerals combined with a multivariate analysis approach, solid-state nuclear magnetic resonance (NMR) enables one to recognize the local structure arrangement of both crystalline and amorphous materials by looking at one or more selected atoms. In present paper targets the ^{13}C nuclide, and thus the major component of marble, calcium carbonate. Whatever their geological origin, marbles ^{13}C-NMR spectra present only one resonance corresponding to the carboxyl function whose intensity and line width vary from one marble to another. If the variation of the NMR signal intensity observed is the result of great T1 variations (from 220 to 5300 s) and is linked to iron content, the line width reflects defects in the calcite crystal in which calcium has been replaced by another element such as magnesium, aluminium or strontium. The specific profile of the NMR signal has been used successfully to help determine the origin of some archaeological items.

KEYWORDS: WHITE MARBLES, PROVENANCE, CULTURAL HERITAGE, NMR, XRD, ICP-OES

INTRODUCTION

Marble was vastly used in plastic art and monumental architecture from the mid-/end of the seventh century BC in ancient Greece: notably to produce the well-known *kouroi* sculptures, but the most famous example is the Parthenon, built in the mid-fifth century BC at the instigation of Pericles. Marble guaranteed the durability and fineness of the finishing, as well as textural homogeneity in sculptural elements and epigraphy. Influenced by Greek culture, marble also became a favourite material in ancient Rome. Soon after it gained control of the Hellenistic kingdoms, Rome imported marble from Greece and Asia Minor and it quickly became a symbol of luxury and power. This boosted the quarrying of previously only locally used marbles, such as that being already exploited in the mid-first century BC (Pliny, 77) in the Apuan Alps near the town of Luna (modern Luni), and currently known as Carrara marble. Its prestige reached its apogee during the reign of the Emperor Augustus, who, according to

*Received 22 June 2018; accepted 12 November 2018

†Corresponding author: email isabelle.pianet@u-bordeaux-montaigne.fr

Suetonius' *Lives of the Caesars* (300), boasted of having found 'a Rome of brick, and left a Rome of marble', and its use spread rapidly from the public to the private sphere and from the centre of the empire to the western territories as they were being conquered, thanks to the *imitatio urbis* phenomenon. Indeed, in the Roman West, the use of marble mirrored the process of Romanization, and with the adoption of Rome's urbanistic and decorative models, marble was intensively sought after to embellish and render monumental the provincial urban centres. This led to the search and exploitation of new marbles sources in these newly conquered territories, and to the import of foreign marbles when the geology did not offer available outcrops. The advantage of local marbles was that their closeness meant having ready available raw material and at a lower cost, since transport had a very high impact on the total price of the material (Antonelli *et al*. 2015; Pensabene 1992). Indeed, recent works clearly prove that the marbles used during antiquity were not exclusively from Greece, Asia Minor or Italy, which as objects of long-distance circulation reached all the corners of the empire, but local sources of less renowned marbles were exploited and distributed owing to an increasing demand for the material, especially the statuary white type.

All this meant that white marbles from very different origins were in use in the same period in the same territories. The importance of the study of marbles is therefore twofold. On the one hand, they provide detailed historical and archaeological data to understand the economics behind the building of the monument or the manufacturing of the artwork or epigraph. On the other, they are also key to comprehending the people and the society that used them, since they give information on trade and economic patterns, as well as the workshops, the human flows involved on the distribution of marbles and those who consumed them. To identify and discover their provenance is, therefore, essential.

Traditionally, more attention has been paid to the provenance of white marble. Great progress has been made on reference databases established through the analysis of marble quarry samples, which are key to discriminate between several ancient quarrying areas and to identify the provenance of archaeological samples. However, certain difficulties still arise regarding the provenance of marbles. Sometimes the results from archaeological marbles fail to match well with the comparative parameters. These discrepancies may be due to multiple causes. On the one hand, new ancient quarries have been discovered both in the east, such as those of Göktepe (near Aphrodisias, Turkey), whose marble shows physical and compositional similarities to Carrara marble (Attanasio *et al*. 2009; Brilli *et al*. 2015; Bruno *et al*. 2015), and in the west, such as those of O-Incio, in the north-western corner of Hispania (Lapuente *et al*. 2014; Gutiérrez Garcia-M. *et al.*, 2016). On the other hand, the use of western marbles on a larger-than-local scale has been confirmed, such as the marbles from the Estremoz Anticline in the Iberian Peninsula (Vidal Álvarez *et al*. 2016) and some French Pyrenean marbles with distribution on both sides of the mountain range (Royo Plumed *et al*. 2015). Moreover, the methods usually applied in the existing reference databases do not always allow discrimination to be made between some of the classical white marbles (Lapuente *et al*. 2014).

This paper proposes to use nuclear magnetic resonance (NMR) spectroscopy, a technique never before applied to the study of ancient marbles. By tracking the ^{13}C nuclide of the most abundant mineral phase of marble, calcite, one can highlight the crystal defects and the presence of trace elements, thus providing a signature for the provenance of marble. The aim is to use this technique to discriminate further between two, or at the most three, possible origins obtained by applying the usual methodology (petrography, cathodoluminescence, X-ray diffraction (XRD), C and O isotopic analyses). The use of NMR in archaeology is over growing due to the development of portable systems and non-invasive practicability (Capitani *et al*. 2012).

MATERIAL AND METHODS

Samples

This study analysed a sample of each of the most relevant white fine-grained marbles used in Roman Spain. Samples included both imperial, imported marbles and local or regional ones. The selected marbles were: Carrara (Apuan Alps, Italy), Göktepe (Karaman province, Turkey), Pentelic (Mount Pentelicus, Greece), Saint-Béat (Midi Pyrénées region, France), Estremoz Anticline (Alentejo, Portugal) and O-Incio (Galicia, Spain).

A small group of three archaeological artefacts was also selected for examination in order to test the reliability of the NMR results. The artefacts consist of objects previously analysed by following the traditional protocols (optical microscopy, cathodoluminescence and isotopic analysis) and, therefore, their provenances were already known. These archaeological pieces were: two portraits, one of the Roman Emperor Hadrian (H), dated from 130 AD, and an unknown female portrait (F), dated from the first to second century AD (both at the National Museum of Tarragona (MNAT) Spain); and the lid of a fifth-century AD sarcophagus dedicated to Ithacius (SI), currently on display at Oviedo Cathedral, Spain. A fourth item was also tested: a contemporary reproduction of a sphinx found at Naxos (S), made in Carrara marble by using a robot. This sphinx is currently located at the entrance of the Maison de l'Archéologie in the Université of Bordeaux-Montaigne (Pessac, France).

In all cases, sampling was carried out on fresh surfaces to avoid any possible weathering effects.

NMR experiments

All samples were powdered with an agate mortar to obtain the 195 ± 5 mg of the powder needed to fill the 4 mm-diameter Cross Polarization Magic Angle Spinning (CP-MAS) rotor. ^{13}C-NMR spectra were recorded on a 400 MHz Bruker Avance II spectrometer equipped with a CP-MAS probe (at the Centre d'Etude Structural et d'Analyse des Molécules Organiques (CESAMO) facilities at the Université de Bordeaux) or on a 850 MHz spectrometer equipped with a MAS probe (at Très Grands Instruments de Recherche- Résonance Magnétique Nucléaire -Très Haut Champ (TGIR-RMN-THC) Fr3050, Très Grands Instruments de Recherche- Résonance Magnétique Nucléaire -Très Haut Champ (CEMHTI) Orléans, France). Two kinds of experiments were performed using a rotation rate of 8000 Hz:

- A simple one-pulse sequence using a 90° nutation angle of 5 µs, a relaxation delay of 300 s, and either 32 or 64 scans (depending on the signal-to-noise ratio of the sample recorded) preceded by two 'dummy' scans to ensure a reproducible pre-saturation of the signal. The same receptor gain was used for all experiments in order to compare the intensity of the signal. No probe back ground signal was removed.
- A saturation-recovery experiment using until 15 inter-pulse delays of between 50 and 1200 s, eight scans, two 'dummy' scans, and a relaxation delay of 1200 s. T1 was obtained using the Bruker software Topspin 3.1 using the following equation:

$$I = I_0\left(1 + P{*}\mathrm{Exp}^{\left(-\frac{\tau}{T1}\right)}\right)$$

where I is the area measured at different τ-values; I_0 the area of the totally relaxed signal; and P is a correcting factor taking into account too short an inter-pulse delay with respect to T1 (Becker *et al.* 1980).

Inductively coupled plasma-optical emission spectrometry (ICP-OES) analyses

A total of 100 mg of each sample were dissolved in a 10 mL solution containing 3 mL HNO_3 68%, 3 mL of HCl 38%, 3 mL of HF 40% and 1 mL of $HClO_4$ 72%. The mixtures were heated for 5 h at 130°C in a closed recipient, and then at 190°C until the total evaporation of all the acids. The remaining powders were disrupted in a 5% HNO_3 solution % before the ICP-OES analysis (720ES, Varian, at the Institut de Chimie de la Matière Condensée de Bordeaux (ICMCB) facilities). The calibration was performed with a mono-elementary standard solution (Aldrich). All the ion contents collected were treated using R software (version 3.3.3), with the *compositions* (version 1.40–1), *FactoMineR* (version 1.36) and *ellipse* (version 0.3–8) packages. Centred log-ratio transformation (CLR) of the compositional data obtained by ICP-OES analysis was performed.

Powder X-ray diffraction (XRD)

Samples were prepared by grinding marbles with an agate mortar and by passing them through a sieve to ensure homogeneity. The XRD patterns were recorded using a Bruker D8 Advance diffractometer, set in Bragg–Brentano reflection mode geometry (CuKα target tube X-ray source, operating at 40 KV and 40 mA). Patterns were obtained by step scans from $2\theta = 3°$ to 60°, with a step size of 0.01° and an acquisition time of 2 s per step. The peaks were indexed by comparing them with powder XRD patterns generated from crystal structures of the Crystallography Open Database (COD; http://www.crystallography.net/index.php). The inclusion of magnesium was calculated by using the strategy reported by Lenders *et al*. (2012).

RESULTS

^{13}C-NMR

Figure 1 displays the ^{13}C-NMR spectra of each quarry sample: only one resonance centred at 170.5 ± 0.1 ppm corresponded undoubtedly to the carbonate function observed. Despite the poorness of these spectra, there are two interesting differences: the intensity of the resonance and its width. These values are reported in Table 1.

Since the amount of marble used to record the spectra was invariably the same (195 ± 5 mg), and the conditions of acquisition were identical (D1, 300 s, number of scans, 64, except for O-Incio marble, for which 32 scans were acquired and the intensity of the signal adjusted (×2), and Receptor Gain, 4600), the variations observed in the signal area must reflect their relaxation behaviour.

The T1 values were measured for each quarry sample using a saturation-recovery experiment. A total of 10–16 different delays were used in a 50–1500 s range (for a total acquisition time of 2–3 days) in order to cover a large T1 value amplitude. Figure 2 displays the evolution of the carbonate signal area of the different marbles according to the recovery delay, τ.

The T1 values calculated from the saturation-recovery experiments are reported in Table 1. Highlighted are significant differences between the marbles depending on their geographical origin in a 200 to $>$ 5000 s range, explaining their specific NMR area response at a fixed inter-pulse delay of 300 s.

The second outstanding characteristic of the ^{13}C-NMR spectra is the full width at half-maximum of the carbonate resonance ($\Delta\nu_{1/2}$; T1): the half width ranges from 50 to $>$ 200 Hz depending on the marble sample. This broadening may be caused either by a distribution of different carbonates (depending on their content of Mg, Fe, Mn or even Sr, which can substitute Ca in the crystal lattice of calcite) and/or by the presence of *para*/ferromagnetic impurities.

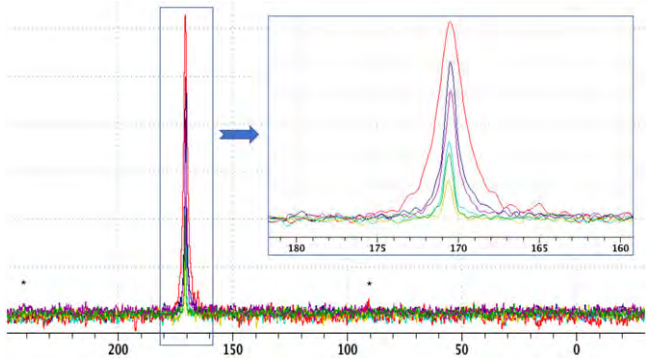

Figure 1 *^{13}C-nuclear magnetic resonance (NMR) spectra of six white marbles from different areas (from the smallest to the highest): Göktepe (yellow), Saint-Béat (green), Carrara (blue), Pentelic (purple), Estremoz Anticline (black) and O-Incio (red). *Rotation side bands. [Colour figure can be viewed at wileyonlinelibrary.com]*

Table 1 *Areas and widths of the ^{13}C resonances of different white marbles from quarries*

			$\Delta\nu_{1/2}$ (Hz)		
Marble origin	*δ (ppm)*	*Signal area*	*100.6 MHz*	*213.8 MHz*	*T1 (s)*
Göktepe	*170.4*	*0.5 ± 0.05*	*50 ± 4*	*n.m.*‡	*5000**
Saint Béat	*170.7*	*1.0 ± 0.07*	*86 ± 4*	*n.m.*	*3000**
Carrara	*170.6*	*1.4 ± 0.10*	*65 ± 5*	*61*	*2000**
Pentelic	*170.5*	*4.1 ± 0.36*	*90 ± 6*	*n.m.*	*500 ± 35*
Estremoz	*170.5*	*4.64 ± 0.07*	*90 ± 10*	*n.m.*	*350 ± 30*
O-Incio	*170.5*	*9.0 ± 0.18*	*210 ± 12*	*274*	*220 ± 25*

*Values ± standard deviation (SD) were calculated as follows: for the signal area, SD was deduced from the signal-to-noise ratio of the recorded spectra (10 for Göktepe, 14 for St Béat, 19 for Carrara, 35 for Pentelic, 45 for Estremoz and 52 for O-Incio); the half-widths were the average of three different values calculated on different spectra at 100.6 or 213.8 MHz; T1 is the average of two different measurements for Pentelic, Estremoz and O-Incio, and were evaluated owing to the acquisition conditions used for Göktepe, St Béat and Carrara.

‡n.m., Not measured.

Recording ^{13}C-NMR spectra at a higher field permits one to distinguish between the two causes of broadening. For this purpose, spectra of Carrara and O-Incio were recorded in a 18.8 T apparatus (at CEMTHI facilities; Table 1). These two marbles were chosen for their line-broadening difference: from 65 for Carrara to 210 for O-Incio at 9.4 T. However, the line width is the same for Carrara, suggesting its high level of purity with respect to calcite; it significantly increases for O-Incio marble (274 Hz), suggesting a higher degree of calcium substitution.

Multi-elemental analysis

The most evident explanation for the ^{13}C-NMR intensity response lies in the elemental content. Paramagnetic species can be responsible for T1 relaxation and the presence of a non-negligible amount of elements may create defaults in the calcite crystal by replacing Ca with another

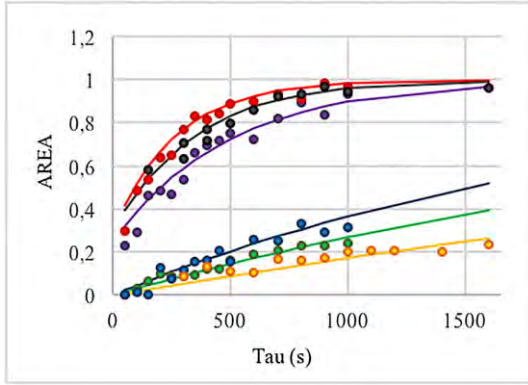

Figure 2 *T1 measurements for white marbles (bottom to top) from Göktepe (yellow), Saint-Béat (green), Carrara (blue), Pentelic (purple), Estremoz Anticline (black) and O-Incio (red). Experimental data (symbols) were fitted using equation 1 (lines). [Colour figure can be viewed at wileyonlinelibrary.com]*

element, notably Mg, to form magnesian calcite crystals. Depending on the original carbonate nature before metamorphism, the elemental trace concentrations can be quite different. This is the case for Göktepe marble, where its aragonite precursor has been recognized as the main cause for its high Sr content (Attanasio *et al*. 2015; Brilli *et al*. 2018). Diagenetic transformations and also fluids circulating during metamorphism could have also caused the introduction of several trace elements into the calcite lattice. Specific impurities, crystal defects and geochemical content on accessory minerals can all be considered responsible for the differences detected in the analysed marbles.

The elements selected for quantification were chosen according to previous studies performed on white marbles from the Piedmont region of Italy (Borghi *et al*. 2009) and from Greece (Mello *et al*. 1988; Ebert *et al*. 2010). On 23 elements first tested (Al, B, Ba, C, Co, Cs, Fe, Li, Mg, Mn, Ni, P, Pb, Rb, Se, Si, Sn, Sr, Te, Ti, Zn and Zr), nine presented more or less discriminant contents according to their geographical location. Thus, Al, B, Fe, K, Mg, Mn, Si, Sr and Ti were measured using ICP-OES (Table 2) and the C content using elementary analysis CHNS (S1).

To visualize the most discriminating elements, a principal component analysis (PCA) was performed in which Ti was removed because of numerous missing values (Fig. 3). The first dimension, which represents 49.62% of the variables, splits Al, Fe and K, on the one hand, and Mg, Mn, Sr and Si, on the other, while the second dimension highlights the role of Si as a discriminant element. However, this analysis shows that the intra-site compositional homogeneity of each quarry site is greater than the possible inter-site similarities. Indeed, so far, each different quarry is well differentiated without significant overlapping, as shown in the scatter plot displayed in Figure 3 (right). This first promising result will obviously be checked with a larger assemblage of quarry samples.

A noteworthy correlation can also be observed between the elemental content and the ^{13}C-NMR signal recorded: while the signal line width ($\Delta\delta$½) is directly proportional to the sum of Mg, Fe, Al, Mn, Mg, Sr and K content ($R^2 = 0.87$; Fig. 4, A), the resonance area is mainly related to the Fe content of the sample ($R^2 = 0.88$; Fig. 4, B).

XRD spectra

Beyond the common uses of XRD in ancient marble studies (i.e., the crystalline phase identification and their relative quantification), we endeavoured to use XRD spectra analysis, and in

Table 2 *Element contents of the different marbles samples from the quarries and archaeological items (F, H, SI, S)*

Element	*Carrara* (n = *2)*	*Estremoz Anticline* (n = *3)*	*O-Incio* (n = *4)*	*Göktepe* (n = *1)*	*Pentelic* (n = *3)*	*St Béat* (n = *4)*	*F*	*H*	*SI*	*S*
Al	117 ± 8	254 ± 18	1691 ± 418	43 ± 6	267 ± 100	124 ± 58	n.d.	97	267	78
B	29 ± 4	29 ± 3	27 ± 6	31 ± 7	29 ± 8	33 ± 10	25	29	21	26
Fe	129 ± 18	228 ± 24	1247 ± 172	55 ± 10	585 ± 120	58 ± 10	19	88	261	88
K	206 ± 4	372 ± 100	1256 ± 106	61 ± 9	202 ± 60	118 ± 50	47	256	336	136
Mg	2674 ± 302	1733 ± 386	3814 ± 152	1186 ± 60	2800 ± 600	1681 ± 400	1291	3096	3895	2365
Mn	28 ± 2	15 ± 7	67 ± 13	n.d.	81 ± 24	68 ± 20	n.d.	17	33	n.d.
Sr	109 ± 7	88 ± 39	267 ± 34	349 ± 10	193 ± 41	187 ± 27	348	102	97	107
Si	239 ± 150	795 ± 106	133 ± 52	385 ± 10	81 ± 27	100 ± 30	193	237	29	662
Ti	11 ± 5	20 ± 2	34 ± 32	12 ± 6	n.d.	n.d.	n.d.	n.d.	17	n.d.

*Values are expressed $\mu g\ g^{-1}$ ± SD (standard deviation).

†n.d., Not detected.

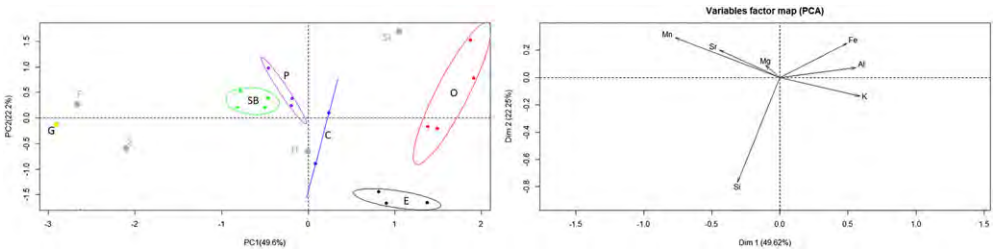

Figure 3 *(left) Principal component analysis (PCA) of geological marbles from Göktepe (G. Yellow), Saint Béat (SB. Green), Carrara (C. blue), Pentelic (P. purple), Estremoz Anticline (E. Black) and O-Incio (O. red); prediction for archaeological items: F, female portrait; H, Hadrian portrait, SI, sarcophagus of Ithacius; and S, sphinx; and (right) variable correlation graph. [Colour figure can be viewed at wileyonlinelibrary.com]*

particular of the diffraction peaks position, to obtain an insight into the chemical disorder in the calcite structure. It is well known that the replacement of Ca^{2+} by Mg^{2+} ions in the crystal lattice of calcite to form magnesian calcite creates changes in the lattice parameters and thus in the position of the diffraction peaks (Meldrum and Hyde 2001). The XRD patterns of the different quarries display a shift of most of the diffraction peaks of the calcite. This is illustrated in Figure 5 (A), which presents the variation of the (104) diffraction peak observed from one sample to another. This phenomenon should be reasonably attributed to calcium substitution by other elements such as Mg, Mn or Sr, as shown by the correlation of [Mg, Sr, Mn] content with the diffraction angle observed for the (104) diffraction peak ([ions] = 28947*(2θ) – 1E+06, $R^2 = 0.73$) (Fig. 5, B). The presence of such chemical disorders in the calcite structure can be partially responsible for the broadening of the ^{13}C-NMR signal due to chemical shift dispersion effects (Fig. 4, A).

Test items

In the first part of this study, we were able to explain the changes observed in the ^{13}C-NMR resonance of samples from different quarries as a consequence of both elemental contents—notably Fe—and defects caused by Ca substitution in the calcite. In this second part, the challenge was to test the applicability of the ^{13}C-NMR to identify the provenance of marbles. For this purpose, some conditions for ^{13}C spectra acquisition were strictly respected: all the spectra were recorded at 195 ± 5 mg with a fixed inter-pulse delay (300 s), a fixed number of scans (64) and a fixed receptor gain (4600).

Figure 6 displays the NMR spectra recorded for all four artefacts and their comparison with six geological marbles which allows one to infer their respective provenance. The almost perfect way in which the observed ^{13}C-NMR spectrum of the female portrait (F) sample is superimposed on the Göktepe sample spectrum suggests it was made with this Turkish marble. The positioning of this item in the PCA analysis (Fig. 3) and the high Sr concentration confirm this provenance (Attanasio *et al.* 2015). The Hadrian portrait (H) presents high similarity with Carrara marble: its ^{13}C-NMR spectrum profile is quite similar to that of Carrara marble, as defined by their characteristic area and line width. The high Mg and low Sr concentrations are in accordance with this attribution as well as its positioning in the PCA graph. The ^{13}C-NMR spectrum of the Ithacius sarcophagus (SI) matches well with the spectrum of Estremoz Anticline marble; while the concentrations in Fe, Sr, K and Al of

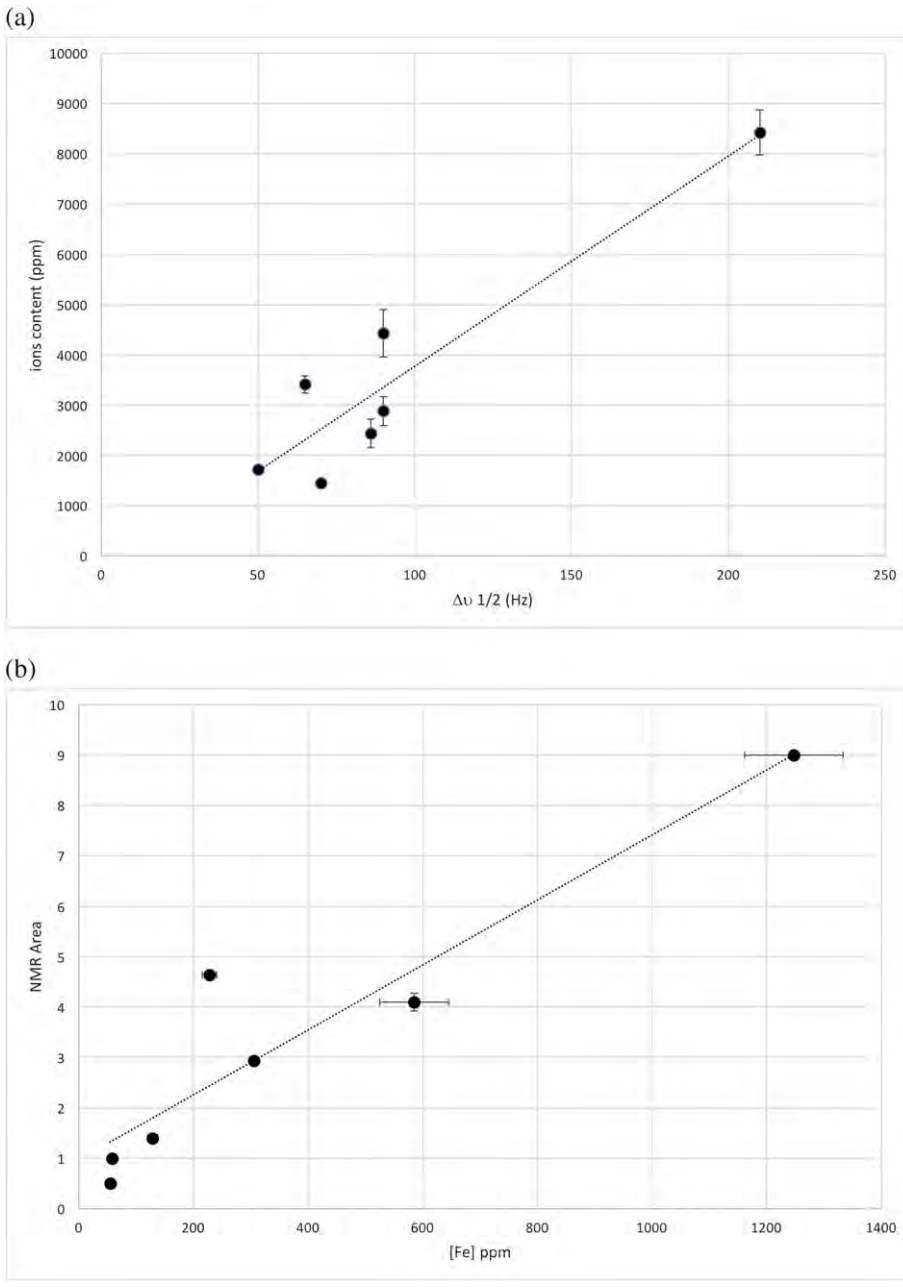

Figure 4 *Correlation between line width ($\Delta\upsilon_{1/2}$) and ion content (A) and between iron content and the nuclear magnetic resonance (NMR) signal area (B). [Colour figure can be viewed at wileyonlinelibrary.com]*

SI are quite similar to those observed in this Portuguese marble, differences can be underlined concerning mainly the Si content, whose determination is tricky. This may explain the peculiar positioning of this item in the PCA analysis, relatively distant from the

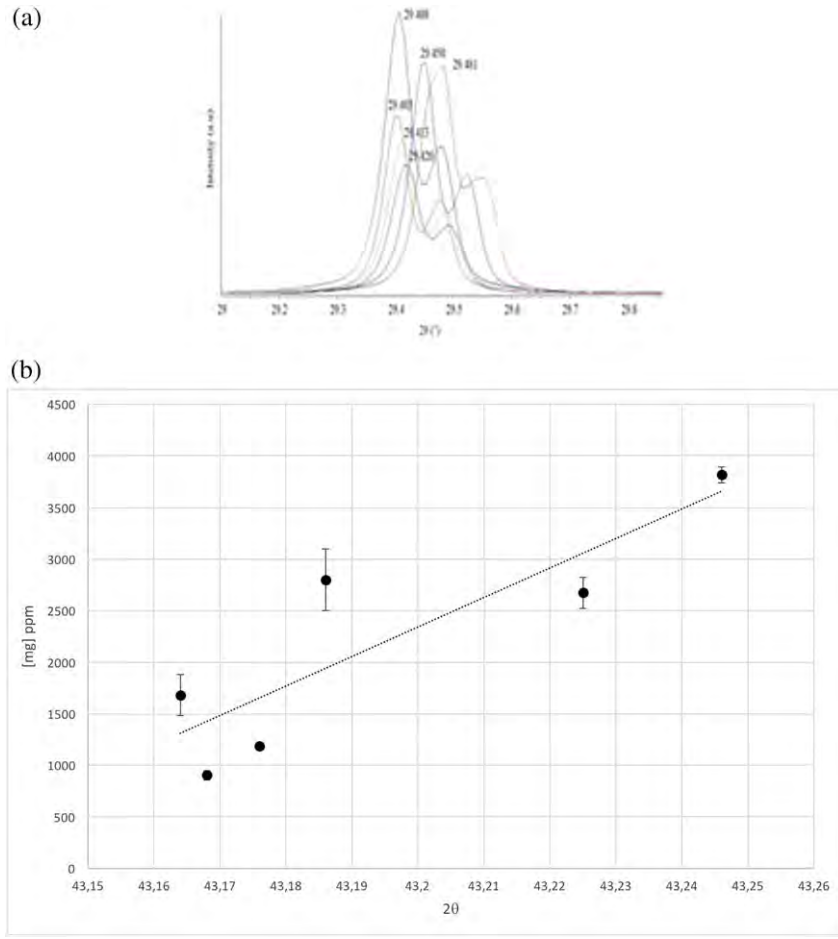

Figure 5 *(A) Powder X-ray diffraction (XRD) of marble samples, in the region of the (104) diffraction peak of calcite, from Göktepe (yellow), Pentelic (purple), Saint Béat (green), O Incio (red), Carrara (blue) and Estremoz Anticline (black); and (B) (104) diffraction peak versus magnesium content. [Colour figure can be viewed at wileyonlinelibrary.com]*

Estremoz Anticline group. Moreover, the highly variable presence of quartz in the Estremoz Anticline marble has been well attested (Lapuente *et al*., 2000). Nevertheless, this attribution for the Ithacius sarcophagus lid was previously proposed thanks to petrographic, cathodoluminescence and isotopic analyses (Vidal Álvarez *et al*. 2016). Lastly, the NMR spectrum of the copy of the sphinx of Naxos, made with Carrara marble, fits perfectly, as expected, with that obtained for this Italian quarrying district. As observed for the sarcophagus of Ithacius, the positioning of the sphinx sample in the PCA plot is far from the delimited region assigned for Carrara marble. Indeed, a detailed analysis of ions content (table 2) evidences again high discrepancies in Si content between the Carrara and sphinx marbles, even if the content of other elements matches (low contents in Fe and Al, and a similar Mg concentration for both).

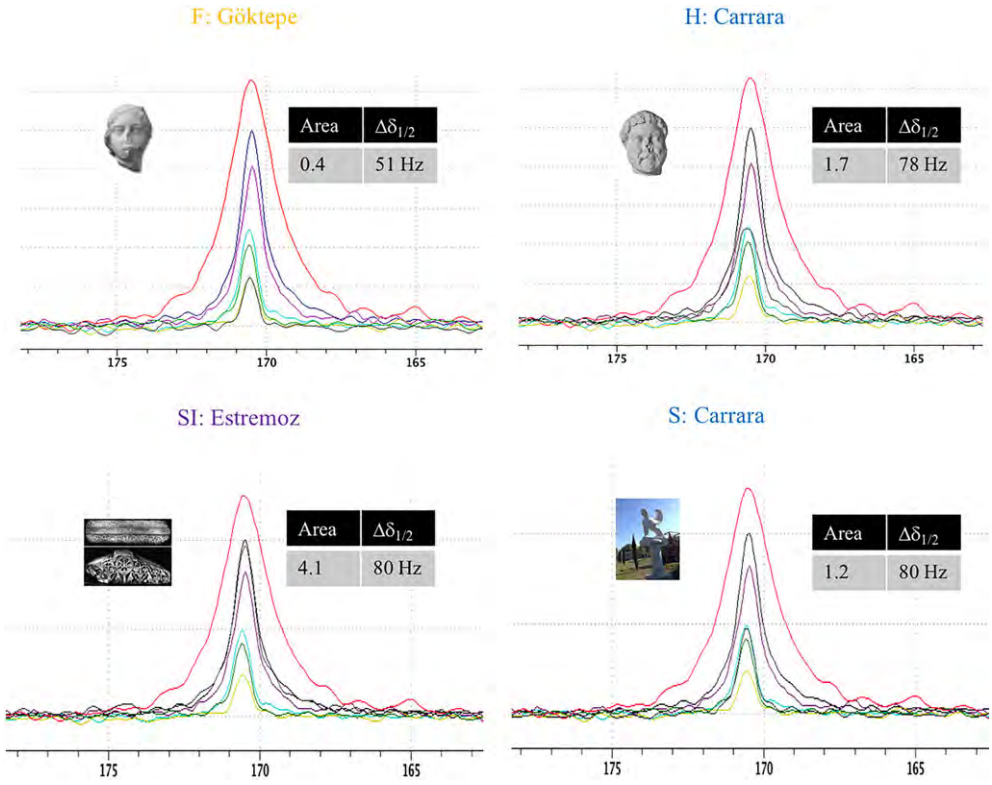

Figure 6 *^{13}C-nuclear magnetic resonance (NMR) spectra of the different archaeological items (grey) and their comparison with the different geological marbles for Göktepe (yellow), Pentelic (purple), Saint Béat (green), O Incio (red), Carrara (blue) and Estremoz Anticline (black). [Colour figure can be viewed at wileyonlinelibrary.com]*

DISCUSSION

Solid-state NMR may provide a powerful tool to ascertain the provenance of archaeological items by tracking intrinsic disorders of geological materials which are a geographical tag. To test the potentiality of ^{13}C-NMR to decipher the geographical origin of marbles, we use the tricky case of white marbles. The marbles studied were chosen with respect to their intensive use during the Roman period, especially in the western part of the empire.

Interestingly, while mainly composed of calcite, as viewed by XRD analyses, all the white marbles present specific ^{13}C-NMR profiles (Fig. 1). These differences are the consequence of the presence of $< 3\%$ secondary elements and their chemical forms in the material. Indeed, some elements such as Mg and Mn, among others, can substitute for the Ca in the calcite crystal, consequently modifying the size of the basic unit cell and the diffraction peaks position (Fig. 5). However, some other chemical species in a crystalline phase such as quartz or micas (see in the supplemental materials) are also present. These 'defects' are likely to be tracked with ^{13}C-NMR and can serve as a discriminant tool: if the signal line width ($\Delta\delta$½) is representative of the total ions content suitable to substitute Ca in the crystal lattice of calcite (Fig. 4, A), the total area of the resonance obtained under given conditions of acquisition, which depends on the T1 relaxation, reflects the Fe content of the sample (Fig. 4, B). These peculiar properties have been exploited in the paper in order to identify the place of origin of the archaeological items and the modern reproduction already

presented. Using the already presented protocol, we have been able to determine or confirm, depending on the considered artefact, the origin of the marble used for their production.

The interest of using NMR spectroscopy is multiple. On the one hand, it requires a very small amount of powered sample, which can also be used for other analyses since NMR is a non-destructive technique. Unlike inductively coupled plasma (ICP) analyses, for example, no previous preparation, which could introduce some bias, is required. In addition, not only can all the chemical species be checked, but also even the amorphous ones; also, numerous nuclei can be analysed on the same sample. Indeed, some ^{43}Ca spectra were acquired for the same samples, giving rise to the different crystalline phases of calcium carbonate and their ratios, especially in the case of the possible presence of dolomite. In this sense, we have carried out some tests with Dolomitic marbles from quarries and from archaeological samples, and the results seem to be promising (Pianet *et al*. 2018).

Obviously, this approach does not exclude all the different methods already used for the identification of white marble origin, which still remain key, such as petrography, cathodoluminescence, and C and O isotopic ratio mass spectrometry. Moreover, given that there is no single analytical technique capable of undoubtedly resolving the provenance of white marble, these first results prove that NMR can greatly contribute to the multi-method approach.

Finally, on the basis of these first very promising results, we intend to check the consistency of spectra within one quarrying district, and thus its applicability to distinguish marbles from different quarries of the same region will be tested in the near future.

ACKNOWLEDGEMENTS

This project was part of the ROMAE project of the LaScArBx (a programme funded by the Agence Nationale de la Recherche (ANR), no. ANR-10-LABX-52) and a collaboration with the project HAR2015-65319-P (MINECO/FEDER) of the ICAC in Tarragona, Spain. NMR analyses were performed at the Centre d'Etude Structural et d'Analyse des Molécules Organiques (CESAMO), ISM, Université de Bordeaux, Département Sciences et Technologie, and the authors thank the CESAMO team, and especially Cybille Rossy, for her help. Some ^{13}C-NMR spectra were collected on the 850 MHz Bruker apparatus thanks to a proposal submitted at the Très Grands Instruments de Recherche- Résonance Magnétique Nucléaire -Très Haut Champ (TGIR-RMN-THC) Fr3050, CEMHTI, Orléans, and the authors thank Pierre Florian for his participation in the analyses. ICP-OES analyses and some XRD experiments were performed at the ICMCB institute, and the authors thank Laetitia Etienne and Stanislav Pechev for their contribution. The authors also thank Ph. Blanc for providing white marble samples from Saint-Béat (Pyrénées). The paper was written through contributions of all authors. All authors gave approval to the final version of the manuscript. AGGM provided archaeological samples and together with RC they are leading the project ROMAE; the results are part of the thesis of MCS on marbles from Galicia. P.L. considerably helped in the preliminary study of petrographic, CL and IRMS data, and oriented the choice of quarries marbles analyses as well as providing samples from Göktepe (Turkey) and Estremoz Anticline area (Portugal). S.P. contributed to the XRD data acquisition and interpretation and prepared all the samples for ICP-OES, NMR and XRD analyses. N.C. contributed to XRD data analyses and performed the ACP analyses. Finally, I.P. managed and wrote up the work.

REFERENCES

Antonelli, F., Lapuente Mercadal, P., Dessandier, D., and Kamel, S., 2015, Petrographic Characterization and Provenance Determination of the Crystalline Marbles Used in the Roman City of Banasa (Morocco): New Data on the Import of Iberian Marble in Roman North Africa, *Archaeometry*, **57**, 405–25.

Attanasio, D., Bruno, M., Prochaska, W., and Yavuz, A. B., 2015, A Multi-Method Database of the Black and White Marbles of Göktepe (Aphrodisias), Including Isotopic, EPR, Trace and Petrographic Data: The black and white marbles of Göktepe (Aphrodisias), *Archaeometry*, **57**, 217–45.

Attanasio, D., Bruno, M., and Yavuz, A. B., 2009, Quarries in the region of Aphrodisias: the black and white marbles of Göktepe (Muğla), *Journal of Roman Archaeology*, **22**, 312–48.

Becker, E. D., Ferreti, J. A., Gupta, R. K., and Weiss, G. H., 1980, The choice of optimal parameters for measurement of spin-lattice relaxation times. II. Comparisaon of saturation recovery, inversion recovery and fast inversion recovery experiments, *Journal of Magnetic Resonance*, **37**, 381–94.

Borghi, A., Vaggeli, C., Marcon, C., and Fiora, L., 2009, The piedmont white marbles used in antiquity: an archaeometric distinction inferred by a minero-petrographic and C-O stable isotope study, *Archaeometry*, **51**(6), 913–31.

Brilli, M., Giustini, F., Conte, A. M., Lapuente Mercadal, P., Quarta, G., Royo Plumed, H., Scardozzi, G., and Belardi, G., 2015, Petrography, geochemistry, and cathodoluminescence of ancient white marble from quarries in the southern Phrygia and northern Caria regions of Turkey: Considerations on provenance discrimination, *Journal of Archaeological Science Reports*, **4**, 124–42.

Brilli, M., Lapuente Mercadal, M. P., Giustini, F., and Royo Plumed, H., 2018, Petrography and mineralogy of the white marble and black stone of Göktepe (Muğla, Turkey) used in antiquity: New data for provenance determination, *Journal of Archaeological Scientific Reports*, **19**, 625–42.

Bruno, M., Attanasio, D., Prochaska, W., and Yavuz, A. B., 2015, An update on the use and distribution of white and black Göktepe marbles from the first century AD to Late Antiquity, in *[ASMOSIA X] Interdisciplinary studies on ancient stone: ASMOSIA X: proceedings of the Tenth International Conference of ASMOSIA, Association for the Study of Marble & Other Stones in Antiquity, Rome, 21–26 May 2012*, 461–468, P. Pensabene, and E. Gasparini, eds., 'L'Erma' di Bretschneider, Rome, Italie.

Capitani, D., Di Tullio, V., and Proietti, N., 2012, Nuclear Magnetic Resonance to characterize and monitor Cultural Heritage, *Progress in Nuclear Magnetic Resonance Spectroscopy*, **64**, 29–69.

Ebert, A., Gnos, E., Ramseyer, K., Spandler, C., Fleitmann, D., Bitzios, D., and Decrouez, D., 2010, Provenance of marbles from naxos based on microstructural and geochemical characterization, *Archaeometry*, **52**(2), 209–28.

Gutiérrez Garcia-M, A., Royo Plumed, H., González Soutelo, S., Savin, M.-C., Lapuente, P., and Chapoulie, R., 2016, The marble of O Incio (Galicia, Spain): Quarries and first archaeometric characterisation of a material used since roman times, *ArcheoSciences Rev A*, **40**, 103–77.

Lapuente Mercadal, M. P., Turi, B., Blanc, P., 2000, Marbles from Roman Hispania: Stable isotope and cathodoluminescence characterization. *Applied Geochemistry*, **15**, 1469–93.

Lapuente, P., Nogales-Basarrate, T., Royo, H., and Brilli, M., 2014, White marble sculptures from the National Museum of Roman Art (Mérida, Spain): sources of local and imported marbles, *European Journal of Mineralogy*, **26**, 333–54.

Lenders, J. J. M., Dey, A., Bomans, P. H. H., Spielmann, J., Hendrix, M. M. R. M., de With, G., Meldrum, F. C., Harder, S., and Sommerdijk, A. J. M., 2012, High-Magnesian Calcite mesocrystals: A coordination Chemistry approach, *Journal of the American Chemical Society*, **134**, 1367–73.

Meldrum, F. C., and Hyde, S. T., 2001, Morphological influence of magnesium and organic additives on the precipitation of calcite, *Journal of Crystal Growth*, **231**, 544–58.

Mello, E., Monna, D., and Odonne, M., 1988, Discriminatting sources of mediterranean marbles: a pattern recognition approach, *Archaeometry*, **30**(1).

Pensabene, P., 1992, Transport, diffusion et commerce des marbres, Le marbre dans l'antiquité - Dossiers d'Archéologie, 86-92.

Pianet, I., A. Gutiérrez Garcia-M, M.-C. Savin, R. Chapoulie, M. P. Lapuente Mercadal, J. Trebosc, and Florian P., 2018, On the provenance of dolomitic white marbles: A natural abondance 43Ca solid-state NMR spectroscopy study., in *ASMOSIA XII, Proceeding of the conference*, ASMOSIA, ed., Izmir, Turquey.

Pliny, 77, *Historia Naturalis*.

Royo Plumed, H., P. Lapuente Mercadal, E. Ros, M. Preite-Martinez, and Cuchi J. A., 2015, Discriminating criteria of Pyrenean Arties marble (Aran Valley, Catalonia) from Saint-Béat marbles: evidence of Roman use, in *[ASMOSIA X] Interdisciplinary studies on ancient stone: ASMOSIA X: proceedings of the Tenth International Conference of ASMOSIA, Association for the Study of Marble & Other Stones in Antiquity, Rome,* 21–6– *May 2012*, 671–682, P. Pensabene, and E. Gasparini, eds., 'L'Erma' di Bretschneider, Rome, Italie.

Suetonius, 300, *Historia Augusta*.

Vidal Álvarez, S., García-Entero, V., and Gutiérrez Garcia-M, A., 2016, La utilización del mármol de Estremoz en la escultura hispánica de la Antigüedad tardía: los sarcófagos, *digitAR*, **3**, 119–28.

SUPPORTING INFORMATION

Additional supporting information may be found online in the Supporting Information section at the end of the article.

Table S1. Elemental analysis. Carbon contents. $CaCO_3$ was purchased from Aldrich, high-performance liquid chromatography (HPLC) quality. Values were obtained from three different measures for two marbles samples, 1 mg of powder to which 3 mg of V_2O_5 were added. The measure was performed on around 1 mg of marble and on a Flash 2000 ThermoFisher CHNS-O apparatus (CESAMO facilities, Talence, France).
Table S2. Carbon contents of some geological marbles (Saint-Béat, Pentelic and O-Incio).
Figures S3–S8. X-ray diffraction (XRD) spectra of the different white marbles showing the presence of different crystalline phases. Figure S8. Difference ^{13}C-nuclear magnetic resonance (NMR) spectra of the four archaeological items.
Figure S2. X-ray diffraction (XRD) spectra of white marble from Carrara showing the presence of different crystalline phases: C, calcite; M, micas; and Q, quartz.
Figure S3. X-ray diffraction (XRD) spectra of white marble from Estremoz Anticline showing the presence of different crystalline phases: C, calcite; M, micas; and Q, quartz, D, Dolomite.
Figure S4. X-ray diffraction (XRD) spectra of white marble from Göktepe showing the presence of different crystalline phases: C, calcite; and Q, quartz.
Figure S5. X-ray diffraction (XRD) spectra of white marble from Paros showing the presence of different crystalline phases: C, calcite; and Q, quartz.
Figure S6. X-ray diffraction (XRD) spectra of white marble from Pentelic showing the presence of different crystalline phases: C, calcite; M, micas; and Q, quartz.
Figure S7. X-ray diffraction (XRD) spectra of white marble from Saint-Béat showing the presence of different crystalline phases: C, calcite; M, micas; and Q, quartz.
Figure S8. Different spectra confirming the origin of marble used for the four archaeological items studied: F, female portrait made with Göktepe marble; H, portrait of Hadrian made with Carrara marble; SI, sarcophagus of Ithacius made with Estremoz Anticline marble; and S, a replica of the sphinx from Naxos made with Carrara marble.